UK public health and ecosystem benefits of currently legislated versus best available emission control measures

Eloise A. Marais[1], Jamie M. Kelly[1,*], Karn Vohra[1], Yifan Li[2], Gongda Lu[1], Naila Hina[3], Ed C. Rowe[3]

[1]Department of Geography, University College London, London, UK.
[2]Reading Academy, Nanjing University of Information Science and Technology, Nanjing, China.
[3]UK Centre for Ecology & Hydrology, Environment Centre Wales, Bangor, UK.
[*]now at: Centre for Research and Clean Air, Helsinki, Finland.

Corresponding author: Eloise A. Marais (e.marais@ucl.ac.uk)

Key Points:

- Efficacy of UK legal and technological control measures tested with emissions projections, GEOS-Chem, and new exposure-harm relationships
- Both reduce public exposure to particulate matter pollution and avoid 6,800 adult early deaths with legislation and 13,300 with technology
- Neither is sufficient at lessening sensitive habitat exposure to harmful loads of nitrogen and concentrations of phytotoxic ammonia

Abstract

Past emission controls in the UK have substantially reduced precursor emissions of health-hazardous fine particles ($PM_{2.5}$) and nitrogen pollution detrimental to ecosystems. Still, 79% of the UK exceeds the World Health Organization (WHO) guideline for annual mean $PM_{2.5}$ of 5 μg m^{-3} and there is no enforcement of controls on agricultural sources of ammonia (NH_3). NH_3 is a phytotoxin and an increasingly large contributor to $PM_{2.5}$ and nitrogen deposited to sensitive habitats. Here we use emissions projections, the GEOS-Chem model, high-resolution datasets, and contemporary relationships between exposure and risk of harm to assess the potential human and ecosystem health co-benefits in 2030 relative to the present day of adopting legally required or best available emission control measures. We estimate that present-day annual adult premature mortality attributable to exposure to $PM_{2.5}$ is 48,625, that harmful amounts of reactive nitrogen deposit to almost all (95%) sensitive habitat areas, and that 75% of ambient NH_3 exceeds levels safe for bryophytes. Legal measures decrease the extent of the UK above the WHO guideline to 58% and avoid 6,800 premature deaths by 2030. This improves with best available measures to 36% of the UK and 13,300 avoided deaths. Both legal and best available measures are insufficient at reducing the extent of damage of nitrogen pollution to sensitive habitats, as most nitrogen emitted in the UK is exported offshore. Far more ambitious reductions in nitrogen emissions (>80%) than is achievable with best available measures (34%) are required to halve excess nitrogen deposition to sensitive habitats.

Plain Language Summary

Particulate matter pollution is detrimental to human health, nitrogen pollution offsets ecosystem balance of sensitive habitats, and ammonia is toxic to plants. Here we determine the potential public health and ecosystem benefits of adopting currently legislated or best available emission control measures. We use state-of-science air quality and exposure assessment models and high-resolution datasets to estimate air pollution abundances and deposition and determine risk of human and ecosystem harm from air pollution in the UK. We find that substantial improvements to public health result from currently legislated measures, estimated as the number of avoided early deaths attributable to decline in particular matter pollution. The number of avoided deaths doubles with best available emission control measures, as these also target particulate matter precursor emissions of ammonia from agricultural activity not mandated by existing legislation. The benefits to sensitive habitats of either legal or best available measures is near-negligible. Mitigating harm to ecosystems will require major advances in emission mitigation technologies.

1 Introduction

Air pollution is a leading global burden of disease (Cohen et al., 2017; Vohra et al., 2021) and is detrimental to ecosystem balance (Sala et al., 2000; Phoenix et al., 2012). In the UK, about 29,000 adult premature deaths have been attributed to long-term exposure to ambient fine particulate matter pollution ($PM_{2.5}$) in a single year (Gowers et al., 2014) and most (70%) sensitive habitats with low nutrient needs are susceptible to harm from deposition of excessive amounts of nitrogen (Rowe et al., 2022). Anthropogenic emissions of ammonia (NH_3), overwhelmingly (~90%) from agriculture, are a large and often dominant component of $PM_{2.5}$ in densely populated cities (Kelly et al., 2023; Vieno et al., 2016) and of nitrogen deposited to ecosystems (Tomlinson et al., 2021). NH_3 is also a phytotoxin (Dise et al., 2011; van Herk et al., 2007; Krupa, 2003).

Measures to reduce NH_3 emissions from agricultural activity in the UK are limited to voluntary implementation of documented best practices (DEFRA, 2018). Over the past 3 decades (1990-2020) anthropogenic NH_3 emissions have declined by just 0.6% a^{-1}; much slower than decline in other $PM_{2.5}$ precursors such as sulfur dioxide (SO_2) at 3.0% a^{-1} and nitrogen oxides (NO_x) at 2.4% a^{-1} (Churchill et al., 2022). NH_3 is a semi-volatile, alkaline gas that partitions reversibly to acidic aerosols forming ammonium (NH_4). Due to sustained controls on local and national SO_2 and NO_x sources, concentrations of acidic sulfate aerosols formed from SO_2 oxidation and acidic nitrate aerosols formed from NO_x oxidation have declined, contributing to decline in NH_4 (Tang et al., 2018). Weakening of the NH_3 aerosol sink and absent controls on agriculture have caused an increase in ambient NH_3 concentrations and the amount of NH_3 deposited to terrestrial ecosystems via dry and wet deposition (Hertel et al., 2012). This has been detrimental to habitats sensitive to excessive nitrogen loads and exposure to NH_3. The latter includes bryophytes, a prevalent class of plants in the UK adversely affected by NH_3 at relatively low concentrations (~1 $\mu g\ m^{-3}$) (Cape et al., 2009).

The UK commits to sustained decline in air pollutant precursor emissions as a signatory of the United Nations Economic Commission for Europe (UNECE) Convention on Long-Range Transboundary Air Pollution (CLRTAP) legislated through the UK National Emission Ceilings Regulations (UK, 2018). The UK met the 2020 targets, according to bottom-up estimates from the National Atmospheric Emission Inventory (NAEI) (Richmond et al., 2020), though top-down NH_3 emissions estimated with satellite observations suggest the NAEI may underestimate NH_3 emissions by 30-50% (Marais et al., 2021). NH_3 emissions targets, reported as percent reduction relative to 2005, are 8% in any year in 2020 to 2029 and 16% from 2030; modest in comparison to SO_2 (59% in 2020-2029 and 79% from 2030) and NO_x (42% in 2020-2029 and 63% from 2030) (Office of the European Union, 2016a). Readily available emission control measures targeting the largest agricultural sources of NH_3, fertiliser use and livestock and manure management (Churchill et al., 2022), include low nitrogen livestock feed, covered manure storage, low emissions methods of spreading manure, filters and scrubbers of air ventilated from animal housing, and low NH_3 alternatives to urea-based fertilisers (Backes et al., 2016). Efficacy of these range from 10-20% decrease in emissions for low nitrogen feed, to 80% decrease for air filtration and covered manure storage, to up to 93% for phasing out urea-based fertilizers (Klimont & Brink, 2004).

Past studies that have assessed separately the public health and ecosystem benefits of emissions controls suggest current measures offer greater benefits to public health than the expense to implement (Giannakis et al., 2019), and that mitigating harm to sensitive ecosystems would require large (at least 40%) reductions in NH_3 emissions (Woodward et al., 2022). Here we investigate whether adoption of measures to meet current legislation or of readily available maximum technically feasible technologies across all sectors, including agriculture, are sufficient to offer combined benefits to public health and sensitive habitats in the UK. We do this by implementing emissions scenarios from the EU's Evaluating the Climate and Air Quality Impacts of Short-Lived Pollutants (ECLIPSE) project (Stohl et al., 2015) in the GEOS-Chem model to simulate the response of ambient $PM_{2.5}$ and NH_3 and nitrogen deposition to emissions changes. We apply these to high spatial resolution datasets of contemporary nitrogen deposition to sensitive habitats and models of the relationship between exposure and risk of harm to calculate adult premature mortality in each UK administrative area and the scale of harm to sensitive habitats.

2 Materials and Methods

2.1 GEOS-Chem Model Description

We use the GEOS-Chem chemical transport model (CTM) version 13.0.0 (https://doi.org/10.5281/zenodo.4618180; accessed 12 December 2021) to simulate present-day and future UK surface concentrations of $PM_{2.5}$ and NH_3 and total (wet and dry) nitrogen deposition due to emissions controls adopted across Europe. The future scenarios are representative of emissions likely in 2030 from adopting either (1) currently legislated emission controls or (2) maximum technically feasible measures. In what follows, the scenarios and associated model results are labelled "PD" for the present-day simulation in 2019, "CLE" for adopting measures to meet current legislation by 2030 and "MTF", also for 2030, but following adoption of maximum technically feasible measures. The model is nested over the UK (49.25ºN to 59.50ºN, 9.375ºW to 3.75ºE) at 0.25º × 0.3125º (28 km latitude × 20 km longitude at the centre of the domain) and is updated 3-hourly with boundary conditions from a global GEOS-Chem simulation at 4º × 5º. The model uses GEOS-FP assimilated meteorology from the NASA Global Modelling and Assimilation Office. All simulations are driven with meteorology for the same year (2019) to isolate the effect of changes in anthropogenic emissions only. The year 2019 instead of 2020 is chosen for the PD simulation, as it is unaffected by the brief, but dramatic decline in emissions resulting from lockdown measures in the first wave of the COVID-19 pandemic in Spring 2020 (Potts et al., 2021).

Anthropogenic emissions in the PD simulation are mostly consistent with those detailed in Kelly et al. (2023) from an earlier model version (v12.1.0) for the same year (2019) used to characterise sources contributing to $PM_{2.5}$ in UK cities. These emissions are from the NAEI for the UK and the European Monitoring and Evaluation Programme (EMEP) for all other European countries. Emissions scaling is applied to terrestrial NAEI and EMEP SO_2 emissions to address a positive bias in modelled SO_2 surface concentrations (Marais et al., 2021) and to NAEI and EMEP NH_3 emissions to resolve differences between bottom-up emissions and those derived with satellite observations of NH_3 column densities (Marais et al., 2021). The scale factors applied are a uniform 60% decrease in land-based SO_2 emissions and 50% increase in NH_3 emissions. The NH_3 emissions scaling is supported by agreement between the model and surface observations of NH_4 concentrations at rural sites throughout the UK with this scaling (Kelly et al., 2023) and, as we show in this work, modelled and observed rainwater concentrations of reduced ($NH_x \equiv NH_3 + NH_4$) nitrogen.

For the future (2030) scenario simulations, we scale anthropogenic emissions in all countries in Europe in the PD simulation using projected changes in emissions derived from integrated assessment models. All anthropogenic emissions, except aviation, are from the ECLIPSE project (Stohl et al., 2015). Emissions due to control measures are predicted in five-year intervals from 1990 to 2050 for multiple major pollutants and precursors (SO_2, NO_x, NH_3, primary $PM_{2.5}$, non-methane volatile organic compounds (NMVOCs), and carbon monoxide) and sectors (agriculture, residential, commercial, energy, industry, on- and off-road transport, shipping, and waste). We use data from the latest version of ECLIPSE (v6b; https://previous.iiasa.ac.at/web/home/research/researchPrograms/air/ECLIPSEv6b.html; last accessed 3 August 2022). For the CLE simulation, we use the ECLIPSEv6b 'CLE' scenario, as this incorporates changes in anthropogenic emissions due to implementation of mitigation

measures legistlated as recently as 2018. For the MTF simulation, we use the ECLIPSEv6b 'MTFR' scenario that assumes adoption of all available air pollution control measures. The ECLIPSEv6b shipping emissions were recently revised to capture a wider range of emission factors for primary particles. Only the CLE emissions were updated, so the same shipping emissions are used for CLE and MTF scenarios. ECLIPSEv6b does not predict aviation emissions, so we take these from Intergovernmental Panel on Climate Change (IPCC) projections downloaded using the Representative Concentration Pathways Database tool version 2.0.5 (https://tntcat.iiasa.ac.at/RcpDb/; last accessed 3 August 2022). The IPCC emissions we use are the business-as-usual Shared Socioeconomic Pathways (SSP) 2-4.5 (Fricko et al., 2017) for the CLE scenario and the sustainable pathways SSP 1-2.6 (van Vuuren et al., 2017) for the MTF scenario. All emissions data are provided as gridded annual values at $0.5^{o} \times 0.5^{o}$, so we derive annual scale factors to apply to PD emissions at $0.5^{o} \times 0.5^{o}$ resolution. Hourly, monthly and seasonal scaling factors are the same as those used for the PD emissions. The Harmonized Emission Component (HEMCO) processing package (Keller et al., 2014) is used to apply scaling factors and to grid emissions to the GEOS-Chem boundary condition and nested model resolutions.

Natural emissions are the same for all scenarios. These are $0.25^{o} \times 0.3125^{o}$ offline emissions of hourly dust (Meng et al., 2021), biogenic VOCs (Weng et al., 2020), and soil NO_x (Weng et al., 2020), and 3-hourly lightning NO_x (Murray et al., 2012). Natural NH_3 emissions are monthly values from the Global Emissions InitAtive (GEIA) inventory for oceans and soils (Bouwman et al., 1997) and annual values from Riddick et al. (2012) for seabirds. GEIA NH_3 emissions are halved to address a known overestimate in these (Paulot et al., 2014).

GEOS-Chem simulates the individual $PM_{2.5}$ components sulfate, nitrate, NH_4, primary and secondary organic aerosols (POA, SOA), black carbon (BC), sea salt, and dust. Formation of sulfate from oxidation of SO_2, detailed in Park et al. (2004), is dominated by in-cloud oxidation by hydrogen peroxide. Formation of aerosol nitrate from uptake of nitric acid (HNO_3) and aerosol NH_4 from reversible partitioning of NH_3 is determined with the thermodynamic equilibrium model ISORROPIA-II (Fountoukis & Nenes, 2007). SOA is estimated with fixed mass yields applied to anthropogenic and biogenic NMVOCs emissions (Pai et al., 2020).

Model representation of other $PM_{2.5}$ components are detailed in Jaeglé et al. (2011) for sea salt and Fairlie et al. (2007) for dust. The proportion of BC and POA emitted as hydrophobic (80% for BC, 50% for POA) ages to hydrophilic at an e-folding time of 1.15 days (Cooke et al., 1999; Chin et al., 2002). Dry deposition is via the Wesely (1989) resistance-in-series scheme. Wet deposition includes scavenging in convective updrafts and rainfall, as well as washout, entrainment and detrainment as detailed in Liu et al. (2001) for water-soluble aerosols and Amos et al. (2012) for gases. We enable the fast scavenging mechanism of Luo et al. (2020) that addresses a positive cold season bias in modelled surface concentrations of aerosol nitrate and NH_4 across Europe. Chemical initialization of the model is achieved with spin-ups of a year for global boundary conditions and 2 months for the PD, CLE and MTF nested domain simulations.

The model is sampled from 1 January to 31 December 2019 to calculate annal mean surface concentrations of NH_3 and components of $PM_{2.5}$ and of reduced and oxidized gas and aerosol-phase nitrogen wet and dry deposition fluxes. Surface concentrations of $PM_{2.5}$ are calculated at standard conditions of temperature (20ºC) and pressure (1 atm) and associated aerosol water is determined using hygroscopic growth factors of individual $PM_{2.5}$ components representative of

50% relative humidity, as detailed in Kelly et al. (2023). Total nitrogen deposition is calculated as the sum of GEOS-Chem deposition fluxes of reduced and oxidized nitrogen compounds that wet and dry deposit (NH_3, NH_4, HNO_3, aerosol nitrates, peroxy acetyl nitrates, and gas-phase organonitrates) and that only dry deposit (NO_2, dinitrogen pentoxide, and C1-C3 alkylnitrates).

2.2 Surface Observations for GEOS-Chem Evaluation

Kelly et al. (2023) compared UK network measurements of $PM_{2.5}$ to $PM_{2.5}$ obtained with an earlier version of the model driven with similar PD emissions to those detailed in Section 2.1. In that comparison, GEOS-Chem annual mean $PM_{2.5}$ is spatially consistent with the observations ($R = 0.66$), but with an expected model underestimate (of 11%), as many of the network sites are in cities along busy roads. We compare our PD model output to that of Kelly et al. (2023) archived on the University College London Data Repository (Marais et al., 2022).

We also evaluate model simulation of nitrogen wet deposition with surface network rainwater concentrations of oxidized and reduced nitrogen. These are from rural and semi-rural UK Eutrophying and Acidifying Pollutants (UKEAP) Precipitation Network (Precip-Net) measurement sites established to determine long-term trends in wet deposition of air pollutants. Data at the forty-one sites operational in 2019 are from the UK-Air data portal (https://uk-air.defra.gov.uk/data/data_selector; last accessed 15 March 2023). Samples at these sites are collected every two weeks to record rainwater volume and measure oxidized (nitrate) and reduced (NH_x) nitrogen rainwater concentrations (Kelleghan et al., 2021). We identify and remove observations contaminated by bird strikes (Conolly et al., 2021) and correct biases in GEOS-FP monthly total precipitation (Neelam et al., 2021; Travis et al., 2016; Paulot et al., 2014). Only three samples are contaminated with bird strikes, identified with phosphate (P) rainwater concentrations > 0.1 mg P L^{-1}. We correct for biases in GEOS-FP precipitation by multiplying GEOS-FP monthly total precipitation (precip) by the correction factor derived by Paulot et al. (2014) ($[precip_{observed}/precip_{modelled}]^{0.6}$), where modelled precipitation is for grids coincident with UKEAP sites. We use the corrected modelled rainwater volume and GEOS-Chem wet deposition fluxes to calculate GEOS-Chem nitrate and NH_x rainwater concentrations.

2.3 Public Health Burden Attributable to Exposure to $PM_{2.5}$

We use the hybrid health risk assessment model from Weichenthal et al. (2022) to calculate adult premature deaths attributable to exposure to $PM_{2.5}$ in the PD and by 2030 due to CLE and MTF control measures. The hybrid model we use merges two functions to represent the relationship between $PM_{2.5}$ and relative risk (RR) of adult (25+ years) premature mortality covering a wide $PM_{2.5}$ concentration range. The functions are known as the extended Shape Constrained Health Impact Function (eSCHIF) and Fusion. eSCHIF was derived with Canadian Census Health and Environment Cohort (CanCHEC) study data covering 2.5 to 17.7 μg m^{-3} (Brauer et al., 2022; Weichenthal et al., 2022). Fusion itself is a hybrid of three widely used health-risk assessment models, established to address deficiencies in each (Burnett et al., 2022). As the Fusion function is underconstrained at very low $PM_{2.5}$ concentrations, Weichenthal et al. (2022) used eSCHIF at 2.5-5 μg m^{-3}, choosing the recently revised World Health Organization (WHO) guideline value of 5 μg m^{-3} (WHO, 2021) to transition between the two curves. This requires an artificial ~14% increase in Fusion RRs at concentrations relevant to the UK to achieve a continuous

curve. We avoid this by rather adapting the code provided by Weichenthal et al. (2022) to transition at the intersection of the two curves at 9.8 μg m^{-3}.

The eSCHIF RR function we apply from 2.5 to 9.8 μg m^{-3} is:

$$eSCHIF(z) = \exp\left\{\frac{\phi \ln\left(\frac{z-z_{cf}}{\alpha}+1\right)}{\left(1+\exp\left(-\frac{z-z_{cf}-\tau}{\upsilon}\right)\right)} + \omega \ln\left(\frac{(z-z_{cf})}{\delta}+1\right)\right\} \quad (1),$$

where z is annual mean $PM_{2.5}$, z_{cf} is the counterfactual concentration of 2.5 μg m^{-3} at and below which RR = 1, and $\phi, \alpha, \tau, \upsilon, \omega$ and δ are best-fit parameters derived from the cohort data. The Fusion curve we apply for $PM_{2.5}$ > 9.8 μg m^{-3} is:

$$Fusion(z) = \exp\left\{\gamma \times (\min(z,\mu) + \int_{\mu}^{z}\left(1+\frac{1-\rho}{\rho}\left(\frac{x-\mu}{\theta-\mu}\right)^{\frac{\theta-\mu}{\theta(1-\rho)}}\right)^{-1} dx + \rho\theta \ln(\max(z,\theta)/\theta))\right\} \quad (2),$$

where γ, μ, ρ and θ are best-fit parameters obtained with the cohort data. $PM_{2.5}$ (z) in Eq. (1) and (2) are PD, CLE and MTF annual means in each GEOS-Chem grid.

Figure 1 shows the shapes of the Fusion and eSCHIF curves and the hybrid of the two for $PM_{2.5} \leq 12$ μg m^{-3}, the peak measured and modelled annual mean $PM_{2.5}$ in the UK in 2019 (Kelly et al., 2023). Fusion is linear at the range relevant to the UK. eSCHIF is supralinear from 2.5 to ~5 μg m^{-3}; a shape supported by epidemiological cohort studies conducted in Europe and North America (Di et al., 2017; Strak et al., 2021).

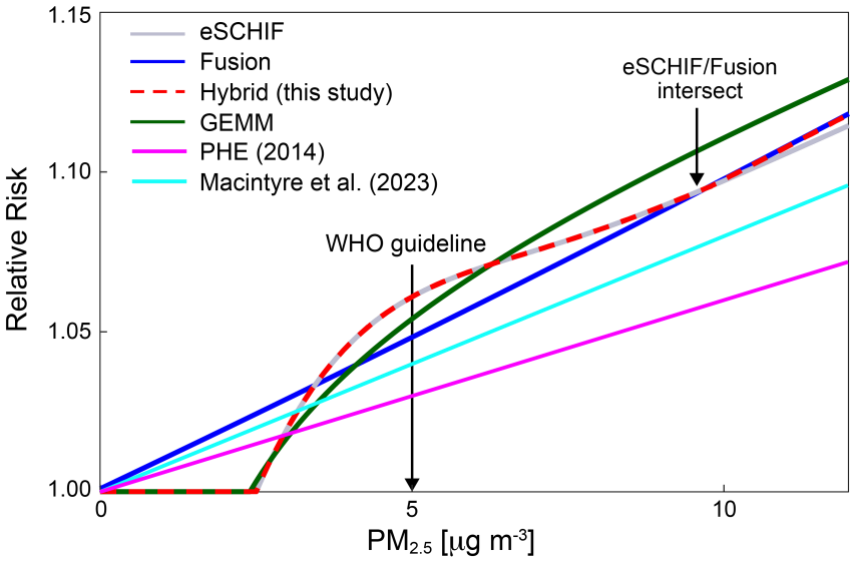

Figure 1. Curves relating relative risk of adult premature mortality to ambient $PM_{2.5}$. Lines are eSCHIF (Eq. (1), grey), Fusion (Eq. (2), blue), the hybrid of the two (red dashed), the Global Exposure Mortality Model (GEMM, green), and curves used in past UK studies by Public Health England (PHE, 2014) (magenta) and Macintyre et al. (2023) (cyan). Arrows point to the WHO 2021 guideline at 5 μg m^{-3} and the intersection of eSCHIF and Fusion at 9.8 μg m^{-3}.

The RR values obtained with Eq. (1) and (2) are used to calculate the fraction of adult nonaccidental deaths attributable to exposure to $PM_{2.5}$, the attributable fraction (*AF*):

$$AF = \begin{cases} 1 - \frac{1}{eSCHIF(z)} & 2.5\ \mu g\ m^{-3} < z \leq 9.8\ \mu g\ m^{-3} \\ 1 - \frac{1}{FUSION(z)} & z > 9.8\ \mu g\ m^{-3} \end{cases} \quad (3).$$

These are calculated for each GEOS-Chem grid and further used to estimate adult excess deaths attributable to exposure to $PM_{2.5}$ as the product of *AF*, adult population, and baseline nonaccidental mortality rates (*BMR*):

$$PM_{2.5}\ \text{excess deaths} = AF \times \text{Adult Population} \times BMR \quad (4).$$

BMRs are from the Global Burden of Disease (GBD) for 2019 to avoid influence from COVID. These are provided in 5-year age increments (https://vizhub.healthdata.org/gbd-results/, last accessed 30 March 2023), where the nonaccidental premature deaths we use are the sum of non-communicable diseases and lower-respiratory infections for adults 25 years and older. These account for 96% of UK total adult premature deaths. *BMRs* are reported for each administrative area in England and at the national scale for Scotland, Wales and Northern Ireland. UK population data for 2019 reported in 5-year age increments at 30 arc-seconds (~1 km) resolution are from WorldPop (https://dx.doi.org/10.5258/SOTON/WP00671; last accessed 5 August 2022). The GBD *BMRs* and cumulative WorldPop data for age-groups 25 years and older are gridded to the GEOS-Chem grid to collocate population and $PM_{2.5}$ pollution hotspots. These gridded data of *AFs*, adult population and *BMRs* are multiplied (Eq. (4)) and the resultant gridded excess deaths are sampled with shapefiles of UK administrative areas (county councils, unitary authorities and metropolitan counties) from the Database of Global Administrative Areas (GADM) (https://gadm.org/; last accessed 17 March 2023). This yields excess deaths in all 184 administrate areas: 119 in England, 32 in Scotland, 22 in Wales, and 11 in Northern Ireland.

We test sensitivity of premature mortality estimates to health-risk assessment model choice by comparing to values obtained with the Global Exposure Mortality Model (GEMM) (Burnett et al., 2018). The GEMM curve, included in Figure 1, is the version obtained without the Chinese Male Cohort, as detailed in Burnett et al. (2018). GEMM is also for adults 25 years and older and has the same counterfactual $PM_{2.5}$ as the hybrid model (RR = 1 at 2.5 μg m^{-3}). GEMM RRs are less than the hybrid model at $PM_{2.5}$ < 7 μg m^{-3} and exceed the hybrid model above this.

2.4 Harm to Nitrogen Sensitive Habitats

We assess the efficacy of emission control scenarios at alleviating harm to sensitive habitats by quantifying the change in the amount and extent of nitrogen deposited in excess of sensitive habitat critical loads and the extent of ambient NH_3 > 1 μg m^{-3} indicative of harm to bryophytes. Recommended habitat-specific critical loads for the thirteen sensitive habitats in the UK are given in Table 1. These range from 5 kg nitrogen (N) ha^{-1} a^{-1} for low resilience habitats such as bogs and montane habitats to 10 kg N ha^{-1} a^{-1} for more resilient habitats such as calcareous grasslands and all woodlands except Scotts pine. These are revised following a recent review (Bobbink et al., 2022) and now 2-7 kg N ha^{-1} a^{-1} less than previously recommended values

compiled by Hall et al. (2015) for all sensitive habitats except the unmanaged oak and other woodlands habitats that are unchanged. We average the critical loads in Table 1 onto the GEOS-Chem grid using maps of fractional coverage of sensitive habitats provided at 1 km resolution by the UK Centre for Ecology and Hydrology (UKCEH). These gridded critical loads are shown in Figure 2(a). Nitrogen sensitive habitats account for 38% of UK land area, dominated by acid grasslands, dwarf shrub heath and coniferous woodlands. Most (58%) of the nitrogen sensitive areas are in Scotland (Rowe et al., 2022). The total coverage in Table 1 of 92,801 km^2 is 973 km^2 less than is in the critical loads trends report compiled by the UKCEH (Rowe et al., 2022), as the GEOS-Chem UK nested domain excludes Shetland Islands.

Table 1. Nitrogen critical loads applied to sensitive habitats in the UK

Sensitive habitat	**Critical load [kg N ha^{-1} a^{-1}] [a]**	**UK coverage [km^2]**	**Contribution [%] [b]**
Acid grasslands	6	20,342	22
Bog	5	8,514	9
Dwarf shrub heath	5	21,496	23
Calcareous grasslands	10	1,012	1
Coniferous woodland	10	14,452	16
Dune grassland	5	631	<1
Deciduous woodland	10	8,706	9
Unmanaged Beech (Fagus) woodland	10	2,059	2
Montane	5	4,915	5
Unmanaged oak woodland	10	6,958	7
Salt marsh	10	808	<1
Unmanaged Scotts pine woodland	5	1,485	1
Unmanaged other woodland	10	1,423	2

[a] Lower end of the range of recently updated values from Rowe & Hina (2023), [b] Percent contribution to UK sensitive area total coverage of 92,801 km^2.

GEOS-Chem is too coarse to resolve deposition to individual sensitive habitats. This is particularly apparent across southern and central England where sensitive habitats account for <20% of GEOS-Chem grid areas (Figure 2(b)). GEOS-Chem wet deposition also does not account for enhanced nitrogen washout from orographic lifting over upland areas (Dore et al., 1992; Fowler et al., 1988). Given this, we use UKCEH Concentration Based Estimated Deposition (CBED) annual multiyear (2018-2020) mean nitrogen deposition rates provided at 5 km resolution to calculate PD nitrogen deposition exceedances. The derivation of this dataset is detailed in Rowe et al. (2022). Briefly, CBED wet deposition fluxes are determined with UK Met Office annual precipitation data and monitoring network observations of ambient reactive nitrogen concentrations and rainwater ion concentrations interpolated to the 5 km CBED grid and by accounting for enhanced wet deposition due to orographic lifting and deposition of cloud droplets to vegetation. Dry deposition is determined with a resistance-in-series model using ammonia concentrations simulated by the EMEP regional CTM at 5 km resolution and vegetation-specific deposition velocities. The CBED deposition data includes nitrogen deposition values for forests and open vegetation. Deposition rates to forests are ~60% more than values for open vegetation,

due to greater surface area of forest vegetation. We map CBED deposition data to the GEOS-Chem grid using UKCEH habitat maps of the spatial coverage of the six woodlands and seven open vegetation habitats in Table 1 before using the gridded deposition data to calculate nitrogen exceedances for the PD. This yields maps of nitrogen deposition in kg N (ha sensitive habitat)$^{-1}$ a^{-1}. We then use GEOS-Chem PD, CLE and MTF total nitrogen deposition to calculate changes in nitrogen deposition due to CLE and MTF emission controls.

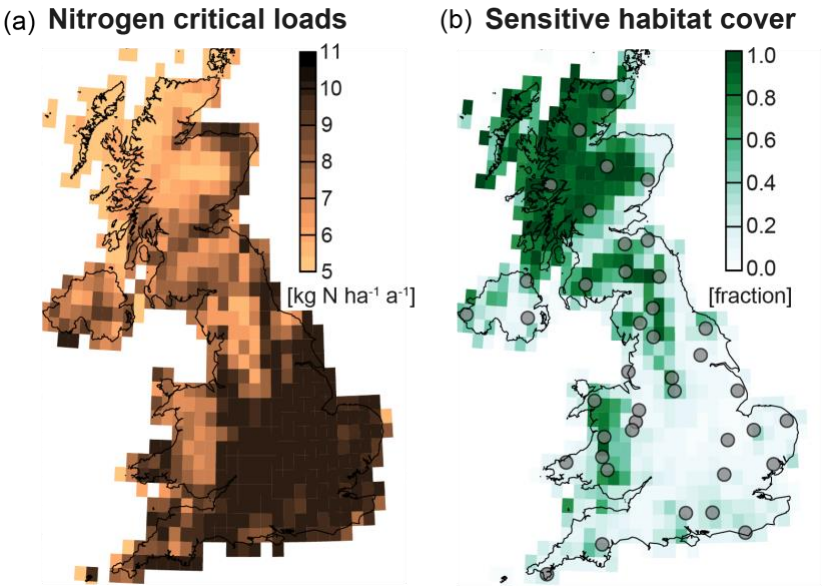

Figure 2. UK nitrogen sensitive habitat critical loads and coverage on the GEOS-Chem grid. Maps are sensitive habitat nitrogen critical loads in kg N (ha sensitive habitat)$^{-1}$ a^{-1} (a) and fractional cover of sensitive habitats in each GEOS-Chem gridcell. Grey circles in (b) are UKEAP Precip-Net monitoring site locations (Section 2.2).

3 Results and Discussion

3.1 Emission Control Scenarios and GEOS-Chem Evaluation

Figure 3 shows annual anthropogenic emissions of NH_3, NO_x, SO_2 and primary $PM_{2.5}$ used in GEOS-Chem PD and future (CLE, MTF) simulations. These are totals for the NAEI domain, so include shipping emissions in UK territorial waters. PD emissions total 452 Gg NH_3, 712 Gg NO_x as NO, 45 Gg SO_2 as S, and 102 Gg primary $PM_{2.5}$. Agriculture accounts for ~90% of anthropogenic NH_3, dominated by fertiliser use and livestock and manure management. NO_x is mostly from land transport and shipping and is the only $PM_{2.5}$ precursor with non-negligible contribution from aviation of 5% in the PD. SO_2 is mostly from industrial processes, energy generation and shipping (Churchill et al., 2022). Primary $PM_{2.5}$ is mostly from residential and commercial sectors and industry.

All air pollutant precursors except NH_3 decline in the CLE scenario by 14% for SO_2, 34% for NO_x, and 24% for primary $PM_{2.5}$. According to ECLIPSEv6b emissions projections, the UK fails to meet its CLRTAP emissions ceilings commitment of 8% decrease in NH_3 emissions with

current measures. Adoption of maximum technically feasible measures surpasses this commitment, achieving a 19% decrease in NH_3 emissions. This is still less than half the minimum decline that Woodward et al. (2022) estimate is needed to significantly mitigate harm to sensitive habitats using less strict critical loads than the updated recommended values (Table 1). The 2% increase in CLE NH_3 emissions in Figure 3(a) is due to limited adoption of suggested measures to offset increase in NH_3 emissions from intensification of agriculture to meet growing food and market demands (Alexandratos & Bruinsma, 2012). NO_x emissions from shipping for both the CLE and MTF scenarios decrease by 21% due to NO_x emissions regulations adopted in the Baltic and North Seas since 2021 (IMO, 2019). Shipping emissions of SO_2 increase by 12% relative to the PD, increasing its contribution to anthropogenic SO_2 emissions from 29% for the PD to 38% for the CLE and 54% for the MTF. According to ECLIPSEv6b, large (>70%) reductions in SO_2 emissions from switching to low-sulfur fuel occur a decade earlier in 2010-2020 (Office of the European Union, 2016b). Aviation NO_x decreases by 19% in the CLE scenario and increases by 10% in the MTF scenario, due to trade-offs between emissions of NO_x and the greenhouse gas carbon dioxide (Freeman et al., 2018; Skowron et al., 2021). The relative contribution of aviation to total NO_x emissions is 7% for CLE and 11% for MTF.

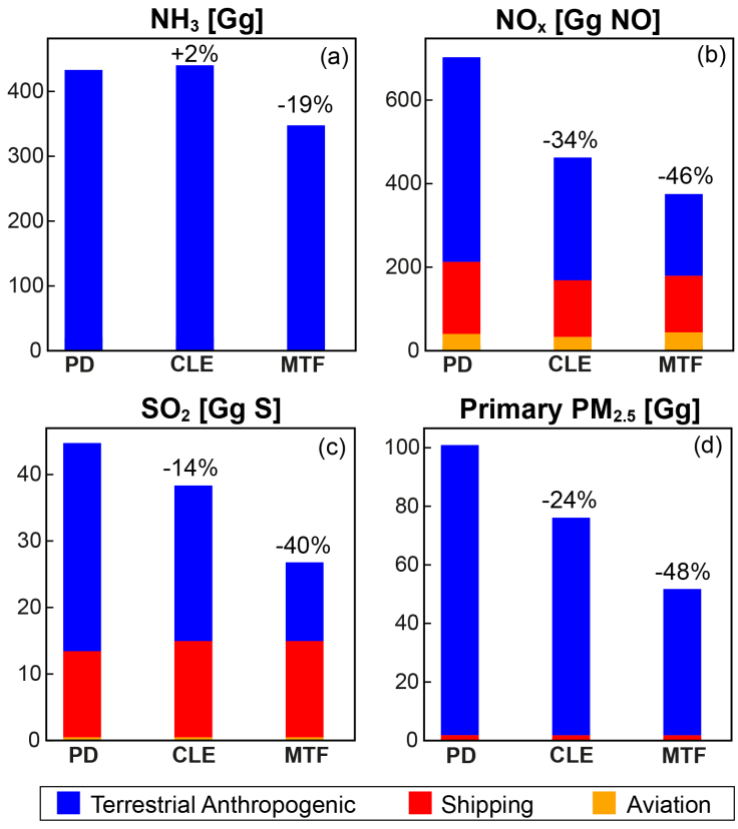

Figure 3: UK present and future anthropogenic emissions of $PM_{2.5}$ and nitrogen pollution precursors. Panels show total annual emissions of NH_3 (a), NO_x (b), SO_2 (c), and primary $PM_{2.5}$ (d) for PD and future (2030) CLE and MTF emissions scenarios. Primary $PM_{2.5}$ is the sum of BC, POA and dust. Inset values are percent change in CLE and MTF relative to PD. Bar colours distinguish surface-bound terrestrial anthropogenic sources (blue), ships (red), and aircraft (yellow).

Figure 4(a) shows GEOS-Chem PD annual mean $PM_{2.5}$. Grids have the same spatial distribution (R = 0.99) and average only 6% or 0.4 μg m^{-3} more than is simulated with the model version from Kelly et al. (2023) (Section 2.2). Monthly UK mean $PM_{2.5}$ in this work ranges from 0.6 μg m^{-3} less (February) to 1.9 μg m^{-3} more (April) than is obtained by Kelly et al. (2023). These differences are due to more efficient cold season wet deposition of nitrate and NH_4 and less extreme downscaling of SO_2 emissions in this work. The latter enhances formation of springtime inorganic sulfate, nitrate and ammonium aerosol. As in Kelly et al. (2023), 79% of GEOS-Chem grids in Figure 4(a) exceed the WHO 2021 annual mean $PM_{2.5}$ guideline of 5 μg m^{-3}.

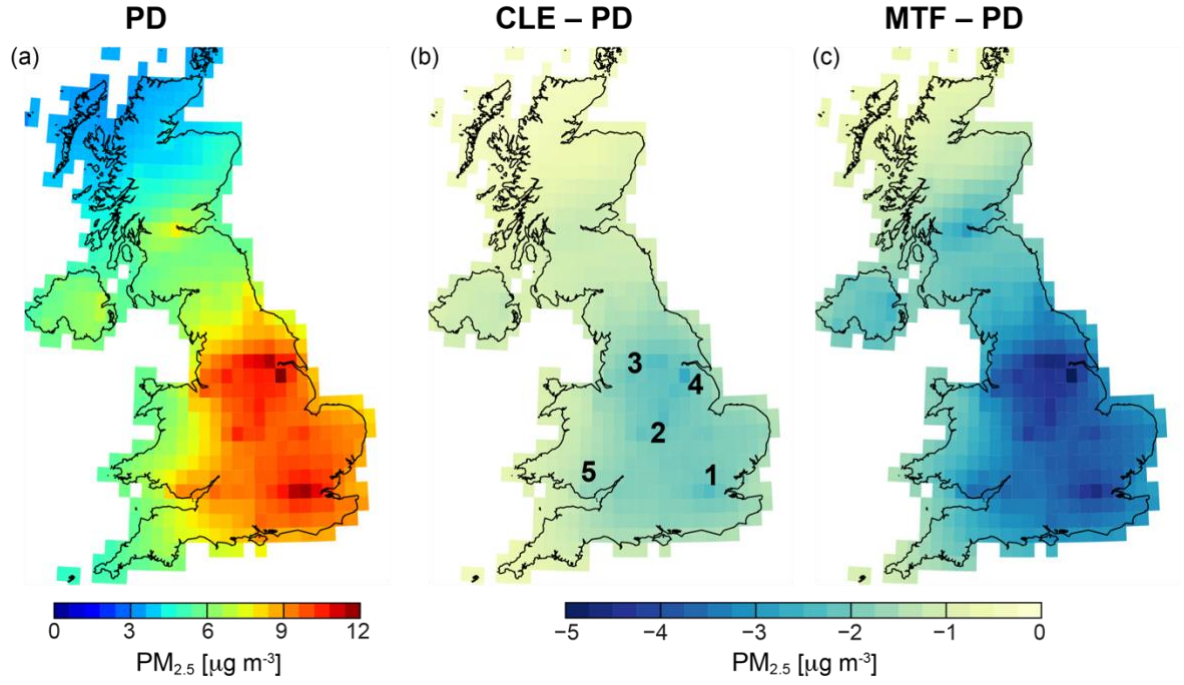

Figure 4. Effect of emission control measures on UK $PM_{2.5}$. Maps are GEOS-Chem annual mean $PM_{2.5}$ in 2019 (PD) (a) and changes in $PM_{2.5}$ relative to the PD due to controls on anthropogenic sources to meet current legislation (CLE minus PD) (b) and adoption of readily available maximum technically feasible measures (MTF minus PD) (c). Inset numbers in (b) are locations with greatest decline in $PM_{2.5}$ discussed in the text: 1. London, 2. Birmingham, 3. Manchester and Leeds, 4. East Yorkshire, and 5. south coast of Wales.

Figure 5 compares observed and modelled rainwater concentrations of nitrate and NH_x to assess GEOS-Chem PD nitrogen wet deposition at UKEAP monitoring sites (Figure 2(b)). Temporal coverage at all sites exceeds 75%. Site mean UKEAP rainwater concentrations are 0.34 mg N L^{-1} for nitrate and 0.42 mg N L^{-1} for NH_x. The correction applied to GEOS-FP total precipitation (Section 2.2) leads to changes in GEOS-FP rainwater volume that varies from a 40-50% increase in December and January, to a 23-26% decrease in April and July, to near-negligible (4-6%) difference in March and November. The overall effect on total rainwater volume in 2019 is a small 4% increase. Without the correction, the correlation between modelled and observed NH_x is weak (R = 0.47) and there is an apparent underestimate in the model of 33% for nitrate and 22% for NH_x. With the rainwater volume correction, both nitrate (R = 0.85) and NH_x (R = 0.64)

399 are spatially consistent, modelled nitrate is 15% or 0.05 mg N L^{-1} less than is observed, and
400 modelled and observed NH_x are equivalent. A 15% difference in oxidized NO_x is more than the
401 prescribed 8% error in NAEI NO_x emissions (Richmond et al., 2020), but in agreement with a low
402 bias in NAEI NO_x emissions when compared to top-down emissions derived with satellite
403 observations of tropospheric columns of nitrogen dioxide (NO_2) (Pope et al., 2022).

404

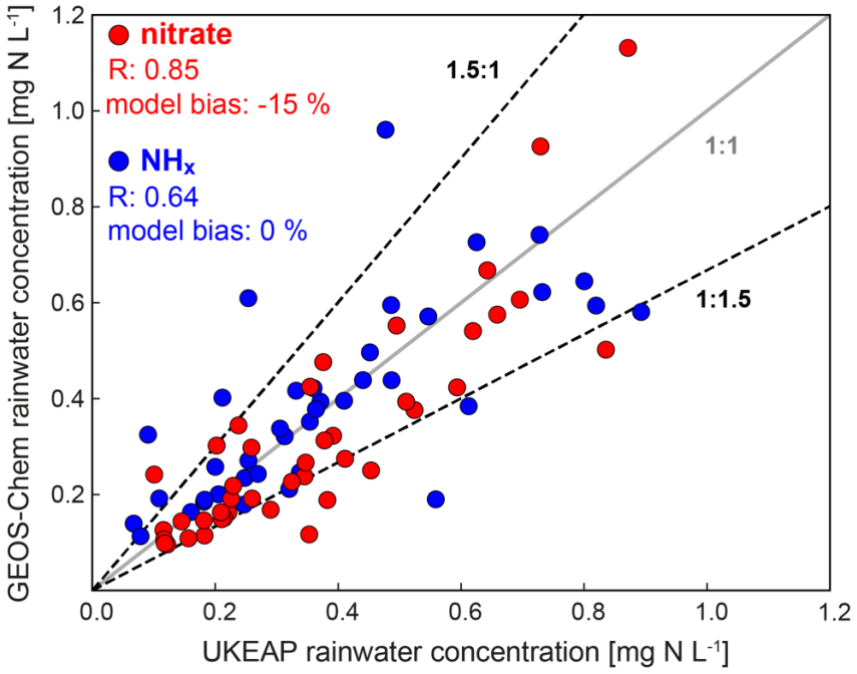

405

406

407 **Figure 5.** Evaluation of modelled nitrogen wet deposition. Scatterplot compares observed
408 (UKEAP) and modelled (GEOS-Chem) rainwater concentrations of oxidized (nitrate, red) and
409 reduced (NH_x, blue) nitrogen at UKEAP sites in 2019. The grey line is the 1:1 relationship and the
410 black dashed lines bound the 50% difference. Numbers inset are the Pearson's correlation
411 coefficient (R) and the model normalized mean bias. Site locations are in Figure 2(b).

412 The contribution of wet deposition to total nitrogen deposition is 58% for grids coincident
413 with UKEAP sites. Many of these sites evaluate model grids dominated by sensitive areas,
414 particularly in Scotland (Figure 2(b)). The 58% contribution to total deposition is similar (57%)
415 for all UK grids and includes contributions from NH_3 (31%), HNO_3 (28%), NH_4 (25%) and aerosol
416 nitrate (15%). The 43% of deposited nitrogen undergoing dry deposition in the UK is mostly (64%)
417 NH_3. There are no network measurements of dry deposition, though dominance of NH_3 has also
418 been inferred from derived dry deposition fluxes obtained using concentration and meteorology
419 measurements and modelled dry deposition velocities at UK monitoring sites (Flechard et al.,
420 2011; Tang et al., 2009).

421 **3.2 Influence of Emission Controls on $PM_{2.5}$ and Public Health**

422 Figure 4 includes the decrease in modelled $PM_{2.5}$ resulting from control measures to meet
423 current legislation (4b) and from adopting maximum technically feasible measures (4c). Decline

in $PM_{2.5}$ in the CLE scenario is at most 2 μg m^{-3} and typically 0.9-1 μg m^{-3}. MTF measures achieve up to 5 μg m^{-3} decline in populated cities (London, Birmingham, Manchester, Leeds) and in locations with intensive industry (Welsh south coast) and large power plants (East Yorkshire). Greater decline in the MTF is due to combined decrease in point source emissions of SO_2, vehicular emissions of NO_x, and agricultural emissions of NH_3 (Figure 3). The largest decline is in April (3.7 μg m^{-3} UK mean) and the smallest is in summer months (1.1-1.5 μg m^{-3}). The percent UK grids in Figure 4(a) that exceed the WHO guideline declines from 79% in the PD to 58% in the CLE and 36% in the MTF. Most of the decline is over Northern Ireland and Scotland north and south of the Central Belt for the CLE and for the MTF this spreads to the rest of Scotland, all of Cornwall and most of Wales.

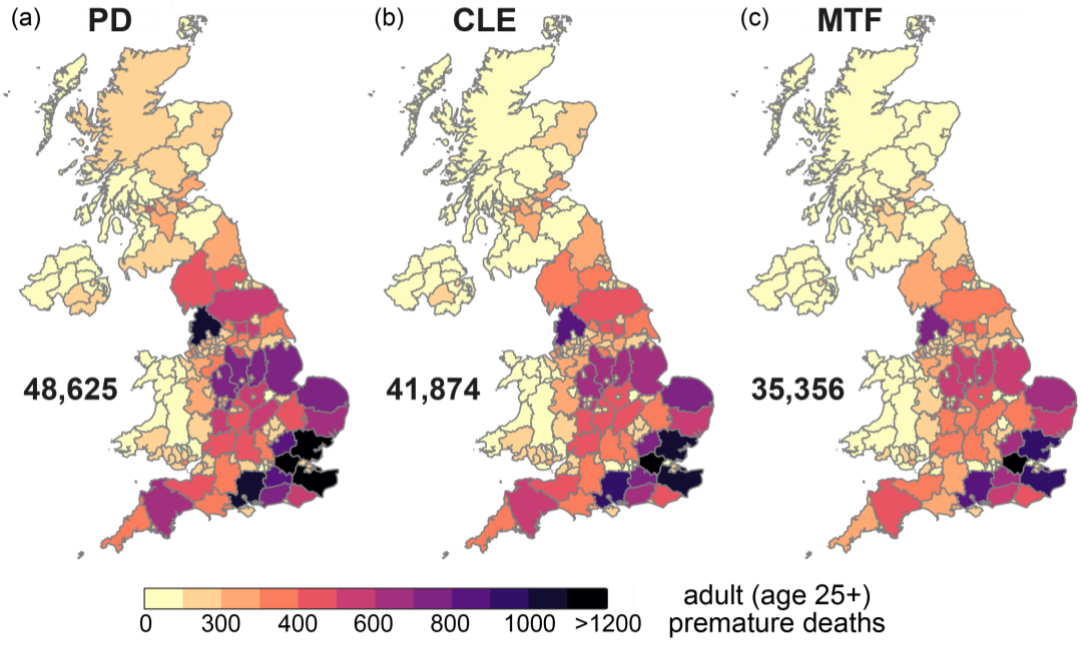

Figure 6. Present-day and future UK adult premature mortality attributable to exposure to $PM_{2.5}$. Maps are administrative area early deaths for the PD (2019) (a) and future (2030) with CLE (b) and MTF (c) emission controls. Inset values are premature mortality estimated with the hybrid eSCHIF-Fusion model detailed in Section 2.3.

Figure 6 maps adult excess deaths attributable to exposure to $PM_{2.5}$ for all 3 scenarios in all UK administrative areas in the PD and by 2030 from adopting CLE or MTF measures. The eSCHIF portion of the hybrid curve (Eq. (1); Figure 1) is applied to 85% of GEOS-Chem grids for the PD and all grids for the CLE and MTF scenarios. $PM_{2.5}$ in all administrative areas exceeds the 2.5 μg m^{-3} threshold for harm in the hybrid model (Figure 1). In the PD, UK annual premature mortality totals 48,625 (95% confidence interval (CI): 45,118-52,595) and on average 8% of premature adult deaths are attributable to exposure to $PM_{2.5}$. Greater London accounts for 10% of these (4,861; 95% CI: 4,549-5,247) and exceeds national totals for Scotland (3,673; 95% CI: 3,214-4,073), Wales (2,462; 95% CI: 2,270-2,660) and Northern Ireland (1,052; 95% CI: 934-1,156). Administrative areas other than Greater London that exceed a thousand excess deaths in the PD are Essex, Kent and Hampshire in southeast England and Lancashire in northwest England.

Lancashire and Hampshire fall below 1,000 with CLE measures and all except Greater London fall below 1,000 with MTF measures.

Annual adult excess deaths for the UK in the PD obtained using GEMM (Figure 1) are 4,608 more than the hybrid model at 53,233 (95% CI: 38,526-67,539), due to higher RRs in GEMM for $PM_{2.5} > 7$ μg m^{-3} typical of populated cities in England (Figure 2(a)). The excess deaths we obtain for the UK in the PD with the hybrid model exceed previously published estimates of 28,969 for 2010 (Gowers et al., 2014) and 40,408 (95% CI: 30,867-45,050) for 2018 (Macintyre et al., 2023). These are both for adults ≥30 rather than ≥25 years old, but this difference has a small effect on burden of disease estimates, as premature mortality for the 25-30 age range is low (PHE, 2014). The curves used in past studies are compared to the hybrid model and GEMM in Figure 1. Incremental changes in risk used in those studies are on average 0.6% (Gowers et al., 2014) and 0.8% (Macintyre et al., 2023) per μg m^{-3} $PM_{2.5}$ or RRs of 1.06 (Gowers et al., 2014) and 1.08 (Macintyre et al., 2023) at 10 μg m^{-3}. The hybrid model change in risk per μg m^{-3} $PM_{2.5}$ ranges from almost 1% for $PM_{2.5} > 9.8$ μg m^{-3} (the Fusion portion of the curve) to 0.5% at 5-9.8 μg m^{-3} and 2.5% at 2.5-5 μg m^{-3}, due to variability in the eSCHIF curve gradient.

Decline in precursor emissions of $PM_{2.5}$ in the CLE results in a UK mean attributable fraction of 7% and total premature deaths of 41,874 (95% CI: 37,949-45,437) by 2030 or 6,751 avoided early deaths. In the MTF, premature deaths attributable to exposure to $PM_{2.5}$ is 6% of all nonaccidental premature deaths and totals 35,356 (95% CI: 29,882-40,015) by 2030. This is 13,269 avoided deaths, representing 27% of PD premature deaths attributable to $PM_{2.5}$ and twice that achieved with current legislation. The GEMM curve also yields a factor of 2 benefit to public health from adopting best available technologies over what is currently legislated.

The elderly (65+) account for most (86%) early nonaccidental deaths in the GBD data, so an aging UK population and recent epidemiological evidence for much greater health risk than the hybrid curve amongst the elderly exposed to $PM_{2.5}$ representative of concentrations in the UK would influence our estimates of avoided deaths. The UK Office of National Statistics projects there will likely be 2.5 million more elderly people in the UK in 2030 than in 2020 (https://www.ons.gov.uk/peoplepopulationandcommunity/populationandmigration/populationprojections/bulletins/nationalpopulationprojections/2020basedinterim; last accessed 2 June 2023), dampening the benefits of emission controls. The causal inference study by Wu et al. (2020) used 16 years of US Medicare data to estimate an RR of at least 1.23 at 10 μg m^{-3} or on average a 2.3% decline in risk per μg m^{-3} decrease in $PM_{2.5}$ amongst the elderly for $PM_{2.5} \leq 12$ μg m^{-3}. This would substantially increase the number of premature elderly deaths attributable to $PM_{2.5}$ in the PD, but also increase the number of avoided early deaths due to emission controls.

3.3 Harm of Nitrogen Deposition and Ambient NH_3 to Sensitive Habitats

GEOS-Chem nitrogen deposited to all UK land totals 253 Gg N in the PD. This is lower than values from higher-resolution models and derived datasets. GEOS-Chem deposition is 25 Gg N or 9% less than is simulated for 2017 with a 5 km resolution CTM (Tomlinson et al., 2021) and 57 Gg N less than gridded mean nitrogen deposition from the CBED dataset (Section 2.4). According to GEOS-Chem, total deposited nitrogen is ~40% of the emitted terrestrial and aviation anthropogenic nitrogen (601 Gg N, Figure 3), suggesting that more than half (~60%) of the nitrogen emitted is exported offshore. As a result, decline in nitrogen deposition by 2030 is only

about a third of the decrease in terrestrial and aviation nitrogen emissions from adopting emission controls. For CLE measures, nitrogen deposited to UK land decreases by 27 Gg N or 31% of the decline in terrestrial and aviation emissions of 88 Gg N (Figure 3). NH_x deposition increases in this scenario by 3 Gg N due to a 2% increase in NH_3 emissions. Decline in UK nitrogen deposition from MTF measures is 75 Gg N or 37% of the 205 Gg N decline in terrestrial and aviation emissions.

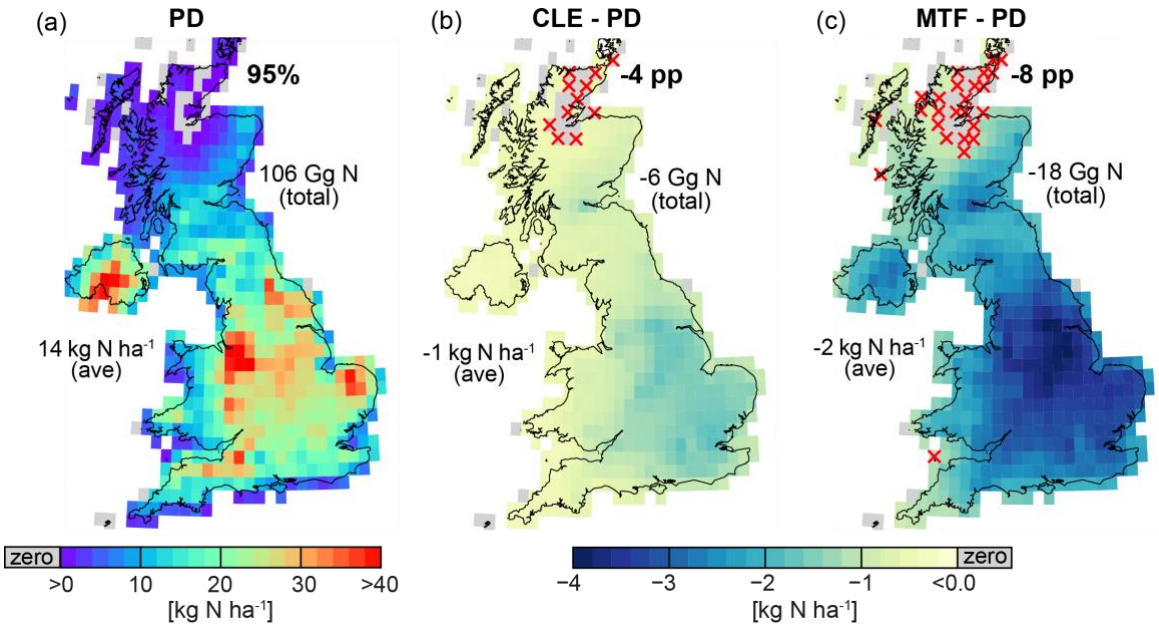

Figure 7. Impact of emission controls on excess nitrogen deposited to UK sensitive habitats. Maps are PD nitrogen deposition above sensitive habitat critical loads obtained with CBED (a) and the change in excess nitrogen deposition resulting from CLE (b) and MTF (c) control measures from GEOS-Chem. All units are kg N (ha sensitive habitat)$^{-1}$ a^{-1}. Grey shaded grids are below critical loads and red crosses identify those that fall below critical lods due to CLE (b) and MTF (c) controls. Inset numbers in (a) are percent UK land area, and total and average excess nitrogen, and in (b) and (c) the change in these relative to the PD. "pp" is percentage point.

Nitrogen deposited to sensitive habitats in excess of critical loads (Figure 2(a)) is shown in Figure 7(a) for the PD (2019). Excess nitrogen covers 95% of sensitive habitats, totals 106 Gg N and averages 14 kg N ha^{-1}. The largest exceedances of >35 kg N ha^{-1} coincide with NH_3 emission hotspots associated with intensive livestock farming (Marais et al., 2021; Hellsten et al., 2008). By 2030, CLE controls decrease total nitrogen deposition to sensitive habitats by 6 Gg N and average exceedances by 1 kg N ha^{-1} (Figure 7(b)) compared to decline of 18 Gg N total and 2 kg N ha^{-1} average decline with MTF measures (Figure 7(c)). For both scenarios, decline in the extent of sensitive habitats exposed to excess nitrogen is modest at 4 percentage points for the CLE and 8 percentage points for the MTF. Almost all this decline is in northern Scotland. A similarly small decline (6 percentage points) is reported for a decade of emission controls from 2010 to 2019 (Rowe et al., 2022). Given that the decline in excess nitrogen deposition is <10% of the decline in emissions, an emissions reduction of at least 500 Gg N may be required to halve excess nitrogen

519 deposition to 50 Gg N. This is ~80% of present-day emissions or more than twice that feasible
520 with best available measures.

521 The extent of UK ambient air with NH_3 concentration > 1 μg m^{-3}, indicative of harm to
522 bryophytes, is 73% in the PD. An increase in UK mean ambient NH_3 in the CLE of 8% increases
523 UK area with NH_3 > 1 μg m^{-3} to 75%. This is due to concurrent increase in NH_3 emissions (Figure
524 3) and decline in the efficacy of the NH_3 acidic aerosol sink (sulfate+nitrate decline by 24%). MTF
525 controls on both NH_3 and acidic aerosol precursor emissions of SO_2 and NO_x (Figure 3) cause
526 decline in both NH_3 (by 13%) and sulfate+nitrate (by 46%), causing a modest decrease in the
527 extent of NH_3 > 1 μg m^{-3} to 69%. As NH_3 is semi-volatile, its emissions depend on multiple
528 environmental factors. A warmer world may, for example, substantially increase NH_3 emissions.
529 One estimate suggests a 5°C warmer world increases global NH_3 emissions by 30-70% (Sutton et
530 al., 2013).

531 **4 Conclusions**

532 Particulate matter pollution even at the relatively low concentrations typical of the UK
533 adversely affect human health and nitrogen pollution harms habitats sensitive to excess deposition
534 and exposure to the phytotoxin ammonia (NH_3). We assess the potential health and ecosystem co-
535 benefits that could be achieved in 2030 following legislative action or from adopting best available
536 emission control measures using emissions projections, the GEOS-Chem model, high-spatial-
537 resolution datasets, and up-to-date relationships between exposure and harm.

538 Legislative measures are most effective at targeting acidic aerosol (sulfate, nitrate)
539 precursor emissions of sulfur dioxide (SO_2) and nitrogen oxides (NO_x), causing decline in fine
540 particulate matter ($PM_{2.5}$) pollution and 6,751 avoided annual early deaths. The extent of the UK
541 above the World Health Organization (WHO) 5 μg m^{-3} guideline for long-term exposure to
542 ambient $PM_{2.5}$ also decreases from 79% to 58%. If instead best available measures are adopted,
543 the number of avoided annual early deaths doubles to 13,269 and less than half (36%) the UK
544 exceeds the WHO guideline.

545 The benefits to habitats are near-negligible for current legislation and modest for adoption
546 of best available measures. Both NH_3 abundance and the amount of nitrogen deposited as NH_3
547 increase with current legislation, as controls on agricultural sources are ineffective at decreasing
548 NH_3 emissions and loss of NH_3 to acidic aerosols declines. Adoption of best available measures
549 decreases NH_3 emissions, as these target major agricultural sources, but these are also insufficient
550 for improving ecosystem health. A far greater (at least 80%) decline in UK nitrogen emissions
551 may be needed to halve harmful nitrogen deposition than the 34% achieved with best available
552 measures.

553 **Author Contributions**

554 EAM conducted the model simulations, analysed the output, calculated the ecosystem harm
555 metrics and led manuscript preparation. JK processed the UKEAP rainwater concentration data
556 and prepared 2050 emissions scalings files. KV calculated premature mortality. YL analysed the
557 emissions data with supervisory support from GLu. GLu also aided in data visualization. NH and

ER provided critical load and CBED deposition data and guided EAM through its use. All co-authors provided editorial input.

Acknowledgements

The authors are grateful to Zbigniew Klimont for guidance on using the ECLIPSEv6b emissions data. This research has been supported by the European Research Council under the European Union's Horizon 2020 research and innovation program (through the Starting Grant awarded to Eloise A. Marais, UpTrop (grant no. 851854).

Conflict of Interest

The authors declare no conflicts of interest relevant to this study.

Data Availability

Data generated as part of this work and that are used, but not available for public access elsewhere, are available on the UCL Data Repository (https://doi.org/10.5522/04/23540079) in NetCDF format. These include GEOS-Chem annual mean ambient $PM_{2.5}$ and NH_3 concentrations and annual total nitrogen deposition, attributable fraction and premature mortality generated with the eSCHIF-Fusion hybrid model, critical loads on the GEOS-Chem grid, UKCEH habitat maps at 1 km resolution, and CBED nitrogen deposition to forests and open vegetation at 5 km resolution. GEOS-Chem version 13.0.0 is preserved at https://doi.org/10.5281/zenodo.4618180 and developed openly on GitHub (https://github.com/geoschem/geos-chem).

References

Alexandratos, N., & Bruinsma, J. (2012). *World agriculture towards 2030/2050: The 2012 revision. ESA Working paper No. 12-03*. Rome, Retrieved from https://www.fao.org/3/ap106e/ap106e.pdf.

Amos, H. M., Jacob, D. J., Holmes, C. D., Fisher, J. A., Wang, Q., Yantosca, R. M., et al. (2012), Gas-particle partitioning of atmospheric $Hg_{(II)}$ and its effect on global mercury deposition, *Atmospheric Chemistry and Physics*, *12*(1), 591-603, doi:10.5194/acp-12-591-2012.

Backes, A. M., Aulinger, A., Bieser, J., Matthias, V., & Quante, M. (2016), Ammonia emissions in Europe, part II: How ammonia emission abatement strategies affect secondary aerosols, *Atmospheric Environment*, *126*, 153-161, doi:10.1016/j.atmosenv.2015.11.039.

Bobbink, R., Loran, C., & Tomassen, H. (2022). *Review and revision of empirical critical loads of nitrogen for Europe*. 358 pp, German Environment Agency (UBA), Retrieved from https://www.umweltbundesamt.de/sites/default/files/medien/1410/publikationen/2022-10-12_texte_110-2022_review_revision_empirical_critical_loads.pdf.

Bouwman, A. F., Lee, D. S., Asman, W. A. H., Dentener, F. J., Van Der Hoek, K. W., & Olivier, J. G. J. (1997), A global high-resolution emission inventory for ammonia, *Global Biogeochemical Cycles*, *11*(4), 561-587, doi:10.1029/97gb02266.

Brauer, M., Brook, J. R., Christidis, T., Chu, Y., Crouse, D. L., Erickson, A., et al. (2022). *Mortality–Air Pollution Associations in Low Exposure Environments (MAPLE): Phase 2*. HEI, Boston, MA, Retrieved from https://www.ncbi.nlm.nih.gov/pmc/articles/PMC9556709/pdf/hei-2022-212.pdf.

Burnett, R., Chen, H., Szyszkowicz, M., Fann, N., Hubbell, B., Pope, C. A., et al. (2018), Global estimates of mortality associated with long-term exposure to outdoor fine particulate matter, *Proceedings of the National Academy of Sciences*, *115*(38), 9592-9597, doi:10.1073/pnas.1803222115.

Burnett, R. T., Spadaro, J. V., Garcia, G. R., & Pope, C. A. (2022), Designing health impact functions to assess marginal changes in outdoor fine particulate matter, *Environmental Research*, *204*, doi:10.1016/j.envres.2021.112245.

Cape, J. N., van der Eerden, L. J., Sheppard, L. J., Leith, I. D., & Sutton, M. A. (2009), Evidence for changing the critical level for ammonia, *Environmental Pollution*, *157*(3), 1033-1037, doi:10.1016/j.envpol.2008.09.049.

Chin, M., Ginoux, P., Kinne, S., Torres, O., Holben, B. N., Duncan, B. N., et al. (2002), Tropospheric aerosol optical thickness from the GOCART model and comparisons with satellite and sun photometer measurements, *Journal of the Atmospheric Sciences*, *59*(3), 461-483, doi:10.1175/1520-0469(2002)059<0461:Taotft>2.0.Co;2.

Churchill, S., Richmond, B., MacCarthy, J., Broomfield, M., Brown, P., Del Vento, S., et al. (2022). *UK Informative Inventory Report (1990 to 2020)*. Retrieved from https://uk-air.defra.gov.uk/assets/documents/reports/cat09/2203151456_GB_IIR_2022_Submission_v1.pdf.

Cohen, A. J., Brauer, M., Burnett, R., Anderson, H. R., Frostad, J., Estep, K., et al. (2017), Estimates and 25-year trends of the global burden of disease attributable to ambient air pollution: an analysis of data from the Global Burden of Diseases Study 2015, *The Lancet*, *389*(10082), 1907-1918, doi:10.1016/s0140-6736(17)30505-6.

Conolly, C., Vincent, K., Sanocka, A., Richie, S., Knight, D., Donovan, B., et al. (2021). *UKEAP 2021 Annual Report*. Retrieved from https://uk-air.defra.gov.uk/assets/documents/reports/cat09/2209290921_2021UKEAP_EA_final.pdf.

Cooke, W. F., Liousse, C., Cachier, H., & Feichter, J. (1999), Construction of a 1° × 1° fossil fuel emission data set for carbonaceous aerosol and implementation and radiative impact in the ECHAM4 model, *Journal of Geophysical Research: Atmospheres*, *104*(D18), 22137-22162, doi:10.1029/1999jd900187.

DEFRA (2018). *Code of Good Agricultural Practice (COGAP) for Reducing Ammonia Emissions*. Retrieved from https://assets.publishing.service.gov.uk/government/uploads/system/uploads/attachment_data/file/729646/code-good-agricultural-practice-ammonia.pdf.

Di, Q., Wang, Y., Zanobetti, A., Wang, Y., Koutrakis, P., Choirat, C., et al. (2017), Air pollution and mortality in the medicare population, *New England Journal of Medicine*, *376*(26), 2513-2522, doi:10.1056/NEJMoa1702747.

Dise, N. B., Ashmore, M., Belyazid, S., Bleeker, A., Bobbink, R., de Vries, W., et al. (2011), Nitrogen as a threat to European terrestrial biodiversity, in *The European Nitrogen Assessment: Sources, Effects and Policy Perspectives*, edited by A. Bleeker, Grizzetti, B., Howard, C. M., Billen, G., van Grinsven, H.,

Erisman, J. W., Sutton, M. A. & Grennfelt, P., pp. 463-494, Cambridge University Press, Cambridge, doi:10.1017/CBO9780511976988.023.

Dore, A. J., Choularton, T. W., Brown, R., & Blackall, R. M. (1992), Orographic rainfall enhancement in the mountains of the Lake District and Snowdonia, *Atmospheric Environment. Part A. General Topics*, *26*(3), 357-371, doi:10.1016/0960-1686(92)90322-c.

Fairlie, T. D., Jacob, D. J., & Park, R. J. (2007), The impact of transpacific transport of mineral dust in the United States, *Atmospheric Environment*, *41*(6), 1251-1266, doi:10.1016/j.atmosenv.2006.09.048.

Flechard, C. R., Nemitz, E., Smith, R. I., Fowler, D., Vermeulen, A. T., Bleeker, A., et al. (2011), Dry deposition of reactive nitrogen to European ecosystems: a comparison of inferential models across the NitroEurope network, *Atmospheric Chemistry and Physics*, *11*(6), 2703-2728, doi:10.5194/acp-11-2703-2011.

Fountoukis, C., & Nenes, A. (2007), ISORROPIA II: a computationally efficient thermodynamic equilibrium model for K^+-Ca_2^+-Mg_2^+-NH_4^+-Na^+-SO_4^{2-}-NO_3^--Cl^--H_2O aerosols, *Atmospheric Chemistry and Physics*, *7*(17), 4639-4659, doi:10.5194/acp-7-4639-2007.

Fowler, D., Cape, J. N., Leith, I. D., Choularton, T. W., Gay, M. J., & Jones, A. (1988), The influence of altitude on rainfall composition at Great Dun Fell, *Atmospheric Environment (1967)*, *22*(7), 1355-1362, doi:10.1016/0004-6981(88)90160-6.

Freeman, S., Lee, D. S., Lim, L. L., Skowron, A., & De León, R. R. (2018), Trading off aircraft fuel burn and NO_x emissions for optimal climate policy, *Environmental Science & Technology*, *52*(5), 2498-2505, doi:10.1021/acs.est.7b05719.

Fricko, O., Havlik, P., Rogelj, J., Klimont, Z., Gusti, M., Johnson, N., et al. (2017), The marker quantification of the Shared Socioeconomic Pathway 2: A middle-of-the-road scenario for the 21st century, *Global Environmental Change*, *42*, 251-267, doi:10.1016/j.gloenvcha.2016.06.004.

Giannakis, E., Kushta, J., Bruggeman, A., & Lelieveld, J. (2019), Costs and benefits of agricultural ammonia emission abatement options for compliance with European air quality regulations, *Environmental Sciences Europe*, *31*(1), doi:10.1186/s12302-019-0275-0.

Gowers, A. M., Miller, B. G., & Stedman, J. R. (2014). *Estimating local mortality burdens associated with particulate air pollution*. Retrieved from https://www.gov.uk/government/publications/estimating-local-mortality-burdens-associated-with-particulate-air-pollution.

Hall, J., Curtis, C., Dore, T., & Smith, R. (2015). *Methods for the calculation of critical loads and their exceedances in the UK*. Retrieved from http://www.cldm.ceh.ac.uk/content/methods-calculation-critical-loads-and-their-exceedances-uk.

Hellsten, S., Dragosits, U., Place, C. J., Vieno, M., Dore, A. J., Misselbrook, T. H., et al. (2008), Modelling the spatial distribution of ammonia emissions in the UK, *Environmental Pollution*, *154*(3), 370-379, doi:10.1016/j.envpol.2008.02.017.

Hertel, O., Skjøth, C. A., Reis, S., Bleeker, A., Harrison, R. M., Cape, J. N., et al. (2012), Governing processes for reactive nitrogen compounds in the European atmosphere, *Biogeosciences*, *9*(12), 4921-4954, doi:10.5194/bg-9-4921-2012.

IMO (2019). Nitrogen Oxides (NO_x) – Regulation 13. Retrieved from: https://www.imo.org/en/OurWork/Environment/Pages/Nitrogen-oxides-(NOx)-%E2%80%93-Regulation-13.aspx.

Jaeglé, L., Quinn, P. K., Bates, T. S., Alexander, B., & Lin, J. T. (2011), Global distribution of sea salt aerosols: new constraints from in situ and remote sensing observations, *Atmospheric Chemistry and Physics*, *11*(7), 3137-3157, doi:10.5194/acp-11-3137-2011.

Kelleghan, D. B., Tang, Y. S., Rowe, E. C., Jones, L., Curran, T. P., McHugh, K., et al. (2021). *National Ecosystem Monitoring Network (NEMN)-Design: Monitoring Air Pollution Impacts across Sensitive Ecosystems*. Retrieved from https://www.epa.ie/publications/monitoring--assessment/air/national-ecosystems-monitoring-network/NEMN-Design_v04-FINAL-(003).pdf.

Keller, C. A., Long, M. S., Yantosca, R. M., Da Silva, A. M., Pawson, S., & Jacob, D. J. (2014), HEMCO v1.0: a versatile, ESMF-compliant component for calculating emissions in atmospheric models, *Geoscientific Model Development*, *7*(4), 1409-1417, doi:10.5194/gmd-7-1409-2014.

Kelly, J. M., Marais, E. A., Lu, G., Obszynska, J., Mace, M., White, J., & Leigh, R. J. (2023), Diagnosing domestic and transboundary sources of fine particulate matter ($PM_{2.5}$) in UK cities using GEOS-Chem, *City and Environment Interactions*, *18*, doi:10.1016/j.cacint.2023.100100.

Klimont, Z., & Brink, C. (2004). *Modelling of Emissions of Air Pollutants and Greenhouse Gases from Agricultural Sources in Europe*. Retrieved from https://pure.iiasa.ac.at/id/eprint/7400/1/IR-04-048.pdf.

Krupa, S. V. (2003), Effects of atmospheric ammonia (NH_3) on terrestrial vegetation: a review, *Environmental Pollution*, *124*(2), 179-221, doi:10.1016/s0269-7491(02)00434-7.

Liu, H. Y., Jacob, D. J., Bey, I., & Yantosca, R. M. (2001), Constraints from Pb-210 and Be-7 on wet deposition and transport in a global three-dimensional chemical tracer model driven by assimilated meteorological fields, *Journal of Geophysical Research-Atmospheres*, *106*(D11), 12109-12128, doi:10.1029/2000jd900839.

Luo, G., Yu, F., & Moch, J. M. (2020), Further improvement of wet process treatments in GEOS-Chem v12.6.0: impact on global distributions of aerosols and aerosol precursors, *Geoscientific Model Development*, *13*(6), 2879-2903, doi:10.5194/gmd-13-2879-2020.

Macintyre, H. L., Mitsakou, C., Vieno, M., Heal, M. R., Heaviside, C., & Exley, K. S. (2023), Impacts of emissions policies on future UK mortality burdens associated with air pollution, *Environment International*, *174*, doi:10.1016/j.envint.2023.107862.

Marais, E. A., Pandey, A. K., Van Damme, M., Clarisse, L., Coheur, P. F., Shephard, M. W., et al. (2021), UK ammonia emissions estimated with satellite observations and GEOS-Chem, *Journal of Geophysical Research-Atmospheres*, *126*(18), doi:10.1029/2021jd035237.

Marais, E. A., Kelly, J. M., Obszynska, J., Mace, M., White, J., & Leigh, R. J. (2022). *GEOS-Chem model output for diagnosing sources of fine particles ($PM_{2.5}$) in UK cities [Dataset]*. doi:10.5522/04/20305401.

Meng, J., Martin, R. V., Ginoux, P., Hammer, M., Sulprizio, M. P., Ridley, D. A., & van Donkelaar, A. (2021), Grid-independent high-resolution dust emissions (v1.0) for chemical transport models:

application to GEOS-Chem (12.5.0), *Geoscientific Model Development*, *14*(7), 4249-4260, doi:10.5194/gmd-14-4249-2021.

Murray, L. T., Jacob, D. J., Logan, J. A., Hudman, R. C., & Koshak, W. J. (2012), Optimized regional and interannual variability of lightning in a global chemical transport model constrained by LIS/OTD satellite data, *Journal of Geophysical Research-Atmospheres*, *117*, D20307, doi:10.1029/2012jd017934.

Neelam, M., Bindlish, R., O'Neill, P., Huffman, G. J., Reichle, R., Chan, S., & Colliander, A. (2021), Evaluation of GEOS precipitation flagging for SMAP soil moisture retrieval accuracy, *Journal of Hydrometeorology*, doi:10.1175/jhm-d-20-0038.1.

Office of the European Union (2016a). *Directive (EU) 2016/2284 of the European parliament and of the Council*. Retrieved from https://eur-lex.europa.eu/legal-content/EN/TXT/PDF/?uri=CELEX:32016L2284&from=EN.

Office of the European Union (2016b). *Directive (EU) 2016/802 of the European Parliament and of the Council of 11 May 2016 relating to a reduction in the sulphur content of certain liquid fuels* Retrieved from https://eur-lex.europa.eu/legal-content/EN/TXT/PDF/?uri=CELEX:32016L0802&rid=1.

Pai, S. J., Heald, C. L., Pierce, J. R., Farina, S. C., Marais, E. A., Jimenez, J. L., et al. (2020), An evaluation of global organic aerosol schemes using airborne observations, *Atmospheric Chemistry and Physics*, *20*(5), 2637-2665, doi:10.5194/acp-20-2637-2020.

Park, R. J., Jacob, D. J., Field, B. D., Yantosca, R. M., & Chin, M. (2004), Natural and transboundary pollution influences on sulfate-nitrate-ammonium aerosols in the United States: Implications for policy, *Journal of Geophysical Research-Atmospheres*, *109*(D15), 20, doi:10.1029/2003jd004473.

Paulot, F., Jacob, D. J., Pinder, R. W., Bash, J. O., Travis, K., & Henze, D. K. (2014), Ammonia emissions in the United States, European Union, and China derived by high-resolution inversion of ammonium wet deposition data: Interpretation with a new agricultural emissions inventory (MASAGE_NH3), *Journal of Geophysical Research: Atmospheres*, *119*(7), 4343-4364, doi:10.1002/2013jd021130.

PHE (2014). *Estimating Local Mortality Burdens associated with Particulate Air Pollution*. Retrieved from https://assets.publishing.service.gov.uk/government/uploads/system/uploads/attachment_data/file/332854/PHE_CRCE_010.pdf.

Phoenix, G. K., Emmett, B. A., Britton, A. J., Caporn, S. J. M., Dise, N. B., Helliwell, R., et al. (2012), Impacts of atmospheric nitrogen deposition: responses of multiple plant and soil parameters across contrasting ecosystems in long-term field experiments, *Global Change Biology*, *18*(4), 1197-1215, doi:10.1111/j.1365-2486.2011.02590.x.

Pope, R. J., Kelly, R., Marais, E. A., Graham, A. M., Wilson, C., Harrison, J. J., et al. (2022), Exploiting satellite measurements to explore uncertainties in UK bottom-up NO_x emission estimates, *Atmospheric Chemistry and Physics*, *22*(7), 4323-4338, doi:10.5194/acp-22-4323-2022.

Potts, D. A., Marais, E. A., Boesch, H., Pope, R. J., Lee, J., Drysdale, W., et al. (2021), Diagnosing air quality changes in the UK during the COVID-19 lockdown using TROPOMI and GEOS-Chem, *Environmental Research Letters*, *16*(5), doi:10.1088/1748-9326/abde5d.

Richmond, B., Misra, A., Brown, P., Karagianni, E., Murrells, T., Pang, Y., et al. (2020). *UK Informative Inventory Report (1990 to 2018)*. Ricardo Energy & Environment, Retrieved from https://uk-air.defra.gov.uk/assets/documents/reports/cat07/2003131327_GB_IIR_2020_v1.0.pdf.

Riddick, S. N., Dragosits, U., Blackall, T. D., Daunt, F., Wanless, S., & Sutton, M. A. (2012), The global distribution of ammonia emissions from seabird colonies, *Atmospheric Environment*, *55*, 319-327, doi:10.1016/j.atmosenv.2012.02.052.

Rowe, E., & Hina, N. (2023). *Empirical critical loads for nutrient nitrogen: defining mapping values for UK habitats. Unpublished report to Defra on National Focal Centre project*. UKCEH.

Rowe, E. C., Hina, N. S., Carnell, E., Vieno, M., Levy, P., Raine, B., et al. (2022). *Trends Report 2022: Trends in critical load and critical load exceedances in the UK.*, UKCEH, Retrieved from https://uk-air.defra.gov.uk/library/reports?report_id=1087.

Sala, O. E., Stuart Chapin, F., Iii, Armesto, J. J., Berlow, E., Bloomfield, J., et al. (2000), Global biodiversity scenarios for the year 2100, *Science*, *287*(5459), 1770-1774, doi:10.1126/science.287.5459.1770.

Skowron, A., Lee, D. S., De León, R. R., Lim, L. L., & Owen, B. (2021), Greater fuel efficiency is potentially preferable to reducing NO_x emissions for aviation's climate impacts, *Nature Communications*, *12*(1), doi:10.1038/s41467-020-20771-3.

Stohl, A., Aamaas, B., Amann, M., Baker, L. H., Bellouin, N., Berntsen, T. K., et al. (2015), Evaluating the climate and air quality impacts of short-lived pollutants, *Atmospheric Chemistry and Physics*, *15*(18), 10529-10566, doi:10.5194/acp-15-10529-2015.

Strak, M., Weinmayr, G., Rodopoulou, S., Chen, J., de Hoogh, K., Andersen, Z. J., et al. (2021), Long term exposure to low level air pollution and mortality in eight European cohorts within the ELAPSE project: pooled analysis, *The BMJ*, doi:10.1136/bmj.n1904.

Sutton, M. A., Reis, S., Riddick, S. N., Dragosits, U., Nemitz, E., Theobald, M. R., et al. (2013), Towards a climate-dependent paradigm of ammonia emission and deposition, *Philosophical Transactions of the Royal Society B: Biological Sciences*, *368*(1621), doi:10.1098/rstb.2013.0166.

Tang, Y. S., Simmons, I., van Dijk, N., Di Marco, C., Nemitz, E., Dämmgen, U., et al. (2009), European scale application of atmospheric reactive nitrogen measurements in a low-cost approach to infer dry deposition fluxes, *Agriculture, Ecosystems & Environment*, *133*(3-4), 183-195, doi:10.1016/j.agee.2009.04.027.

Tang, Y. S., Braban, C. F., Dragosits, U., Simmons, I., Leaver, D., van Dijk, N., et al. (2018), Acid gases and aerosol measurements in the UK (1999–2015): regional distributions and trends, *Atmospheric Chemistry and Physics*, *18*(22), 16293-16324, doi:10.5194/acp-18-16293-2018.

Tomlinson, S. J., Carnell, E. J., Dore, A. J., & Dragosits, U. (2021), Nitrogen deposition in the UK at 1 km resolution from 1990 to 2017, *Earth System Science Data*, *13*(10), 4677-4692, doi:10.5194/essd-13-4677-2021.

Travis, K. R., Jacob, D. J., Fisher, J. A., Kim, P. S., Marais, E. A., Zhu, L., et al. (2016), Why do models overestimate surface ozone in the Southeast United States?, *Atmospheric Chemistry and Physics*, *16*(21), 13561-13577, doi:10.5194/acp-16-13561-2016.

UK (2018). *The National Emission Ceilings Regulations 2018 (No. 129)*. Retrieved from https://www.legislation.gov.uk/uksi/2018/129/made/data.pdf.

van Herk, C. M., Mathijssen-Spiekman, E. A. M., & de Zwart, D. (2007), Long distance nitrogen air pollution effects on lichens in Europe, *The Lichenologist*, *35*(4), 347-359, doi:10.1016/s0024-2829(03)00036-7.

van Vuuren, D. P., Stehfest, E., Gernaat, D. E. H. J., Doelman, J. C., van den Berg, M., Harmsen, M., et al. (2017), Energy, land-use and greenhouse gas emissions trajectories under a green growth paradigm, *Global Environmental Change*, *42*, 237-250, doi:10.1016/j.gloenvcha.2016.05.008.

Vieno, M., Heal, M. R., Williams, M. L., Carnell, E. J., Nemitz, E., Stedman, J. R., & Reis, S. (2016), The sensitivities of emissions reductions for the mitigation of UK $PM_{2.5}$, *Atmospheric Chemistry and Physics*, *16*(1), 265-276, doi:10.5194/acp-16-265-2016.

Vohra, K., Vodonos, A., Schwartz, J., Marais, E. A., Sulprizio, M. P., & Mickley, L. J. (2021), Global mortality from outdoor fine particle pollution generated by fossil fuel combustion: Results from GEOS-Chem, *Environmental Research*, *195*, doi:10.1016/j.envres.2021.110754.

Weichenthal, S., Pinault, L., Christidis, T., Burnett, R. T., Brook, J. R., Chu, Y., et al. (2022), How low can you go? Air pollution affects mortality at very low levels, *Science Advances*, *8*(39), doi:10.1126/sciadv.abo3381.

Weng, H., Lin, J., Martin, R., Millet, D. B., Jaeglé, L., Ridley, D., et al. (2020), Global high-resolution emissions of soil NO_x, sea salt aerosols, and biogenic volatile organic compounds, *Scientific Data*, *7*(1), doi:10.1038/s41597-020-0488-5.

Wesely, M. L. (1989), Parameterization of surface resistances to gaseous dry deposition in regional-scale numerical models, *Atmospheric Environment*, *23*(6), 1293-1304, doi:10.1016/0004-6981(89)90153-4.

WHO (2021). *WHO global air quality guidelines: particulate matter ($PM_{2.5}$ and PM_{10}), ozone, nitrogen dioxide, sulfur dioxide and carbon monoxide*. Retrieved from https://apps.who.int/iris/handle/10665/345329.

Woodward, H., Oxley, T., Rowe, E. C., Dore, A. J., & ApSimon, H. (2022), An exceedance score for the assessment of the impact of nitrogen deposition on habitats in the UK, *Environmental Modelling & Software*, *150*, doi:10.1016/j.envsoft.2022.105355.

Wu, X., Braun, D., Schwartz, J., Kioumourtzoglou, M. A., & Dominici, F. (2020), Evaluating the impact of long-term exposure to fine particulate matter on mortality among the elderly, *Science Advances*, *6*(29), doi:10.1126/sciadv.aba5692.